

On the Microstructure and Wear Behavior of Fe–xCr–4Mn–3C Hardfacing Alloys

Yogesh Kumar Singla^{1,2} · Rahul Chhibber³ · Navneet Arora¹ ·
Karanpreet Singh² · Kishore Khanna²

Received: 19 February 2016 / Accepted: 18 August 2016 / Published online: 2 September 2016
© The Indian Institute of Metals - IIM 2016

Abstract The present paper describes an investigation aimed at evaluating the microstructural and dry sliding adhesive wear characteristics of Fe–xCr–4Mn–3C hardfacing alloys applied through shielded metal arc welding. The effect of chromium addition on the microstructure of hardfacings was carried out by using optical microscope, field emission scanning electron microscope and X-ray mapping. Dry sliding wear tests were performed on a pin-on-disc wear tribometer. From the experimental results, it was observed that the primary carbides were refined and increased with the increase of chromium content. The morphology of carbides revealed that the primary carbides were rod shaped. The increased chromium content was also found to be beneficial to enhance hardness and wear resistance of hardfacings. The correlation between hardness and wear resistance exhibited the reliability of hardness as an indicator of the wear performance of hardfacings.

Keywords Dry sliding wear · Microstructure · M_7C_3 carbide

1 Introduction

Many engineering components are subjected to various modes of wear including abrasive, adhesive, erosive, impact-sliding, etc. To protect the components from wear damage, hardfacing is an effective method being used widely. Cheaper iron based alloys with chromium and carbon or relatively expensive alloys with some niobium or titanium have long been used as standard hardfacing materials [1]. Among all the coating processes available, welding is the simplest and generally the most well-known method. Unlike other processes, welding requires no specific surfacing equipment, since any existing equipment can be used to surface the materials. The only specific need is the utilization of correct consumables [2]. The incorporation of alloying elements into the weld overlays is relatively easy in shielded metal arc welding (SMAW) process [3]. The literature review indicates that researchers have also used the pre-placement technique for depositing the hardfaced weld overlays through the tungsten inert gas welding process [4–9].

Iron based alloys are most widely used as hardfacing materials with relatively high percentages of chromium and carbon. The microstructures of such alloys are composed of alpha ferrite and complex carbides, which makes the matrix harder and resistant to wear [5]. Previous studies reported that the austenitic matrix with high volume fraction of M_7C_3 carbides result in the excellent abrasive wear resistance of hardfacing alloys [9]. However, many factors such as the type, shape and distribution of hard phases, as well as the toughness and strain hardening characteristics of the matrix also play an important role in determining the abrasion resistance of hardfacing alloys [10]. Singla et al. [11] have studied the effect of load and grit size on the abrasive wear of iron based hardfacing alloys having

✉ Yogesh Kumar Singla
yogesh12360@gmail.com

¹ Mechanical and Industrial Engineering Department, IITR, Roorkee, Uttarakhand 247667, India

² Mechanical Engineering Department, Thapar University, Patiala, Punjab 147004, India

³ Mechanical Engineering Department, IITJ, Jodhpur, Rajasthan 342011, India

variation in their chromium contents. A number of uni-directional wear tests have been conducted by various researchers to report the wear behavior of the material [12–17].

Fe–Cr–C alloys having carbon 2–5 wt% and chromium 18–30 wt% show the existence of M_7C_3 carbide. These microstructures possess excellent wear resistance properties [18–21]. Apart from this, the presence of a large volume fraction of M_7C_3 carbides has also shown good wear resistant properties [22–27]. In addition, in previous studies, Fe–Cr–C alloy has already been proved to be the most promising alloy in modifying the tribological properties of bulk materials [28, 29]. Therefore, in the present paper, chromium has been varied in different proportions to investigate its effect on the microstructure, hardness and dry sliding adhesive wear characteristics of Fe–xCr–4Mn–3C alloys. An attempt has also been made to correlate the microstructural changes with the hardness and wear resistance of hardfacings.

2 Experimentation

2.1 Materials and Welding Conditions

Low carbon steel plates (mild steel) having dimensions $265 \times 125 \times 12 \text{ mm}^3$ were used for hardfacing purpose by means of shielded metal arc welding process. The chemical composition of the steel plate was measured by optical emission spectrometer (Metavision-1008i) and is presented in Table 1.

A total of six hardfacing tubular electrodes having variation in their chromium content were formulated. Hardfacings were deposited on the substrate in flat position. Prior to welding, the electrodes were baked in a furnace at a temperature of 100 °C for 2 h. Three hardfacing layers were deposited in order to examine the top layer without the influence of significant dilution effects. The inter-pass was maintained at 200 °C for the deposition of adjacent beads. On completion of weld depositions, the hardfacings were allowed to cool in the air at ambient temperature. The welding parameters used to prepare the weld surfacing were as follows: welding current 140–160 A; voltage 21–23 V and speed 2–3 mm/s (approx.).

The hardfaced deposit chemistry was determined on the top of the weld deposit by utilizing an optical emission spectrometer and is listed in Table 2. A minimum level of

5 wt% was selected, since, Dasgupta et al. [30] published that the wear resistance of iron based alloys could only be improved with a chromium content of more than 3 wt%.

2.2 Metallography, Hardness, XRD and Dry Sliding Wear Tests

A water cooled abrasive cutting machine was used to cut hardfaced alloys. Metallography test specimens were then prepared using the standard polishing procedure followed by cloth polishing. The polished specimens were etched with Vilella's reagent consisting of one part of HNO_3 , two parts of HCl and three parts of glycerol. Microstructures were examined with optical microscope (Leica DM I500 M, Germany) and field emission scanning electron microscope (FE-SEM, 200 Quanta FEI). The qualitative and quantitative description of elemental variations in the weld overlays were performed using EDS (200 PENTA FET Precision) compositional maps and EDS analysis respectively. X-ray elemental mapping was also carried out to show the distribution of alloying elements in the matrix.

Bulk hardness of the hardfacings and substrate was measured on a Vicker's hardness testing machine (Amsler Otto Moplert-Werke GMBH D-6700, Germany) under a constant load of 5 kg using 136° diamond pyramid indenter. The average hardness of 10 reading has been reported in the present study.

2.3 Dry Sliding Wear Test

A pin-on-disc wear testing apparatus (Ducom India, Model: TR-201LE-M8) was utilized to investigate the wear characteristics of hardfacings and substrate. The pins of dimensions having 30 mm length and 8 mm diameter were prepared as per ASTM standard guidelines [31]. Prior to wear test, the specimens were polished against a silicon carbide abrasive paper of 600 grit size to a surface roughness of approximately $R_a 0.56 \mu\text{m}$ and then cleaned with acetone. An electronic weighing balance (Shimadzu Japan, Model: AUW 220) with $\pm 0.1 \text{ mg}$ accuracy was utilized to weigh the specimens. To perform wear tests under dry sliding conditions, specimens were held against EN32 steel disc of 200 mm diameter under a constant load of 70 N. Sliding distance was varied from 400 to 2800 m in six steps with an increment of 400 m. Table 3 illustrates the dry sliding wear testing conditions used in the present study.

Table 1 Chemical composition of low carbon steel plate

Elements	C	Si	Mn	P	S	Cu	Nb	Cr	Fe
wt%	0.18	0.21	0.4	0.08	0.06	0.06	0.004	0.052	Balance

Table 2 Chemical composition of weld deposits

Elements	Weight percentage of constituents					
	Hardfacing 1	Hardfacing 2	Hardfacing 3	Hardfacing 4	Hardfacing 5	Hardfacing 6
Mn	4.281	4.101	4.513	4.122	4.167	4.243
C	3.121	3.197	3.547	3.314	3.024	3.466
Cr	4.875	8.903	12.758	16.819	20.793	24.914
Fe	Balance	Balance	Balance	Balance	Balance	Balance

Table 3 Sliding wear test details at a glance

Parameters	Values
Test apparatus	Pin-on-disc
Specimen's roughness	$R_a = 0.36 \mu\text{m}$
Sliding distance	400, 800, 1200, 1600, 2000, 2400, 2800 m
Sliding speed	800 RPM
Normal load	70 N
Counter disc	Material: EN-32, diameter: 200 mm, hardness: 63–65 HRC
Lubrication condition	Dry
Relative humidity	50.6 %
Temperature	Ambient (25 °C approx.)

The wear rate was calculated from the weight loss technique and was expressed in terms of grams per meter. Prior to weighing, the specimens were cleaned with acetone.

3 Results and Discussion

3.1 Hardfacing Microstructures

The typical optical micrographs of chromium additive hardfacing alloys are shown in Fig. 1. From Fig. 1a–f, it is seen that the microstructure of hardfacings are overlaid with a number of carbides, which increases with the increase of chromium content. In Fig. 1a, when chromium addition is 5 wt%, carbide visibility is very poor, in fact, it seems that no carbide has formed. This is due to the fact that chromium amount is not sufficient to react with carbon to form chromium carbide. With the increase of chromium from 5 to 9 wt%, carbides begin to appear in the microstructure (Fig. 1b) and exhibit an increase in 13 wt% Cr additive alloy. Further, hardfacings containing 17, 21 and 25 wt% chromium, comprises of a network of both primary carbides in the form of long spine-like blades and hollow hexagons, which indicates that the carbides are rod-shaped. The results are consistent with the previously reported literature [32–37]. A careful examination shows that the increase in chromium content has no significant

effect on the morphology of primary carbides (Fig. 1d–f). But the primary phase seems to be refined and hole defects decreases. The existence of hole defects in the primary carbides is attributed to solidification of liquid melt into the eutectic structure. In view of this, Ohide and Ohira [38] stated that when the primary carbides are formed, primary hexagonal shells surround the hypereutectic liquid and when the primary carbides are growing, the hexagonal shells thicken continuously. Finally, liquid melt solidifies into the eutectic structure, which become hole defect in the primary carbide. Buchely et al. [39] reported that the primary carbides grow almost perpendicular to the wear resistant surface and this orientation is beneficial in enhancing the wear resistance. The primary carbides are expected to be M_7C_3 carbides as previous literature reports have stated that the primary carbides in chromium rich alloys are of M_7C_3 type [13, 19, 29, 32, 34–37, 40–43]. High magnification SEM image of 25 wt% chromium additive alloy (Fig. 2a), EDS (Fig. 2b) and X-ray mapping analysis (Fig. 2c–h) confirms that the primary carbides are of M_7C_3 type. Quantitative analysis of the marked position 1, reveals that carbides are mainly chromium and iron rich and a prominent peak of Fe and Cr can also be identified from EDS analysis (Fig. 2b). Therefore, M_7C_3 carbides include Cr_7C_3 and Fe_7C_3 . Li et al. [44] and Atamert and Bhadeshia [45] carried out the phase diagram calculation of high chromium cast iron and documented that the main primary carbide was M_7C_3 . The elemental distribution (Fig. 2c–g) and their mixture (Fig. 2h) show that all the elements are distributed uniformly into the matrix. From Fig. 2c, it can be noticed Fe is distributed mainly in the eutectic structure. Figure 2d shows that Cr is distributed mainly in the primary phase and a small amount of it is distributed in the eutectic structure. Figure 2e–g shows that Si, C and Mn are dispersed throughout the scanning area. Figure 2h shows the mixture of all alloying elements at a glance.

It has been stated that during the solidification process, primary M_7C_3 carbides are formed, followed by the eutectic reaction $[L-CrFe + (Cr,Fe)_7C_3]$ [4]. Therefore, the primary M_7C_3 carbides and fine eutectic colonies of austenite and smaller M_7C_3 are obtained in hardfacing alloys. In addition,

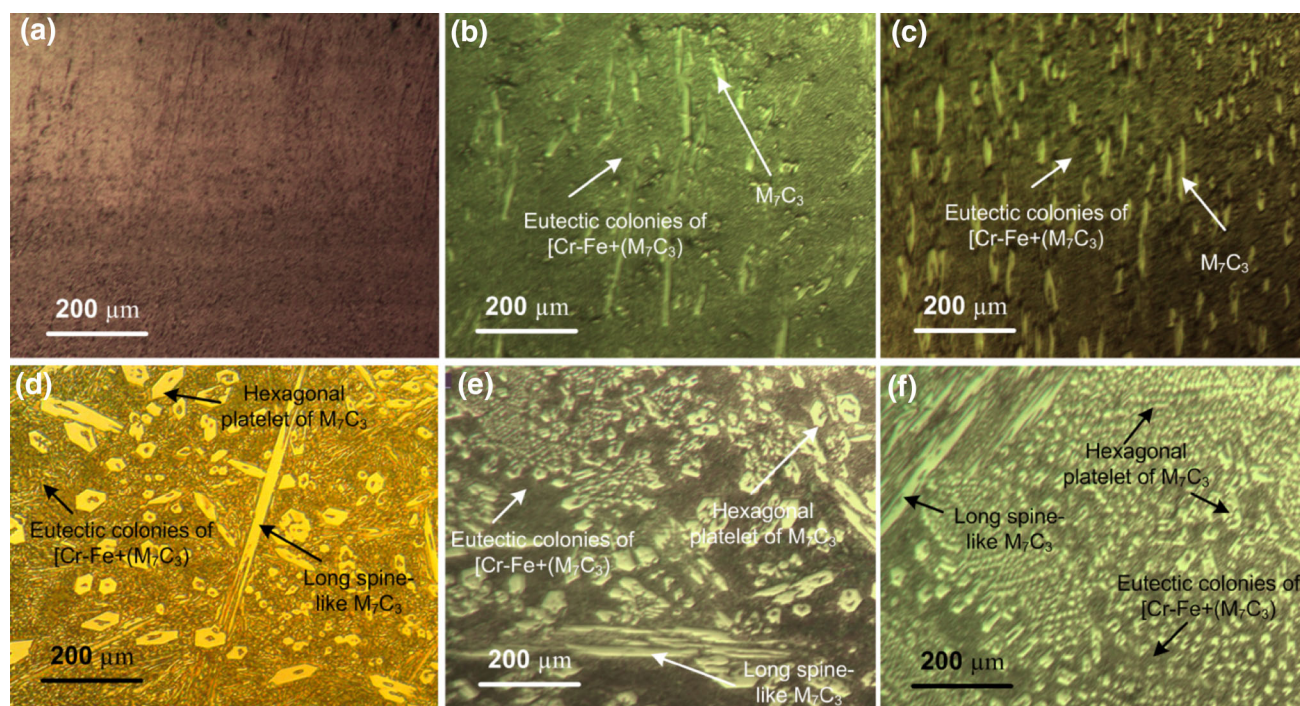


Fig. 1 Optical micrographs of hardfacings **a** Cr-5 wt%, **b** Cr-9 wt%, **c** Cr-13 wt%, **d** Cr-17 wt%, **e** Cr-21 wt%, **f** Cr-25 wt%

microstructural examination also reveals that there is no evidence of cracks, defects, unmelted particles and porosity in the hardfacings.

The average hardness values (along with the standard deviation) of substrates and hardfacings are illustrated in Fig. 3.

From Fig. 3, it is seen that the increased chromium content directly influences the hardness of hardfacings and increases linearly with the increase of chromium content. When chromium is 5 wt%, hardness is minimum and reaches a maximum of approximately 700 VHN with 25 wt% chromium addition. The increase in hardness is associated with a higher amount of hard M_7C_3 carbides, favoured by high chromium in comparison to other chromium additive hardfacings. The hardness of primary carbides has been reported to range between 1300 and 1800 VHN [46] and is much higher than that of the eutectic matrix [47]. Apart from this, the microstructural analysis reveals that the distribution of carbides become dense and uniform with the increase of chromium addition. This is indicative of an increased area fraction of carbides. Based on the above discussion, it can be concluded that the increase of hardness is mainly attributed to the refinement of carbides accompanied by the increased area fraction of carbides.

3.2 Dry Sliding Wear Characteristics

The typical wear behaviour of substrate and hardfacings can be visualized from the Fig. 4.

From Fig. 4, it is seen that the wear rate decreases with the increase in sliding distance. The initial stages give steep rise to greater wear, which corresponds to the run-in-wear. Run-in-wear is the unstable fluctuations between the two surfaces when they meet each other and it usually occurs at the start of the sliding. This may be attributed to the mechanical welding of the plastically deformed material at the edges of the pin and is characterized by plastic and elastic deformation in the areas with the greatest roughness until the steady-state friction regime is reached [48, 49]. The plateau in the wear rate curves represents the establishment of the constant wear rate after initial sliding. Graphical presentation shows that the steady state stage of the wear rate curves is reached after a sliding distance of 800 m.

The wear rate of substrate is higher than that of the hardfacings. Among six hardfacings, hardfacing 6 exhibits a minimum wear rate. The enhanced wear resistance of hardfacing 6 is attributed to the high hardness caused by the increased area fraction of carbides. The result indicates that more area fraction of carbides is beneficial in improving the wear resistance of hardfacings. This is because, the increased contents of hard primary M_7C_3 carbides provide a barrier against the indentation, grooving and cutting. The increased carbide area fraction does not always reduce the wear, sometimes, it may also result in spalling and fracture of carbides, if formed beyond a certain limit and can accelerate the wear rate. In the present study, the reduction in wear rate is an indication of better

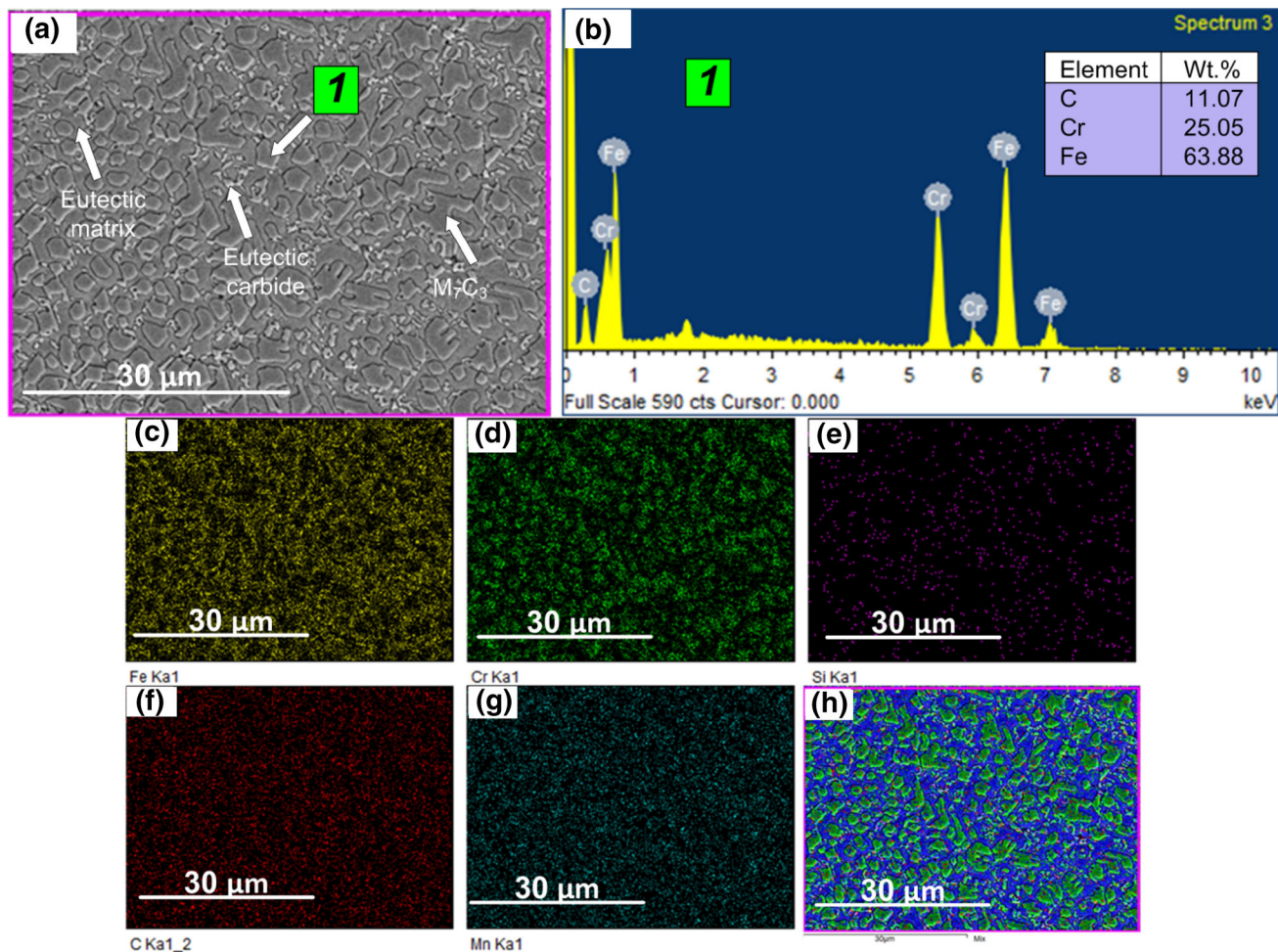


Fig. 2 Cr-25 wt% a SEM image, b EDS analysis, c–g X-ray mapping of individual element, h mixture of all elements

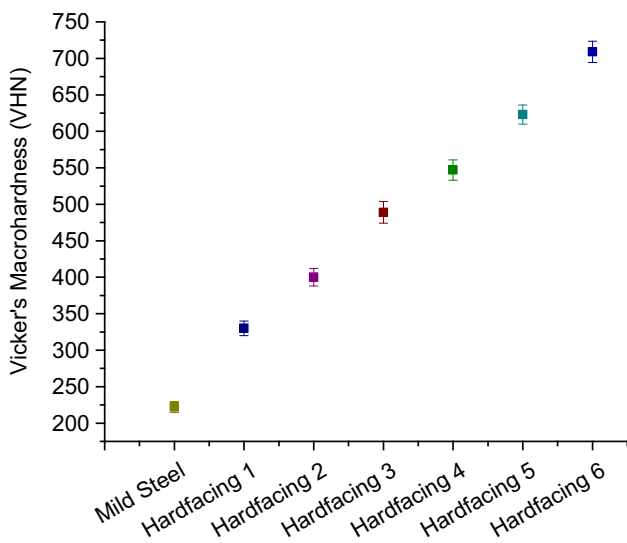


Fig. 3 Macrohardness of substrate and chromium additive hardfacing alloys

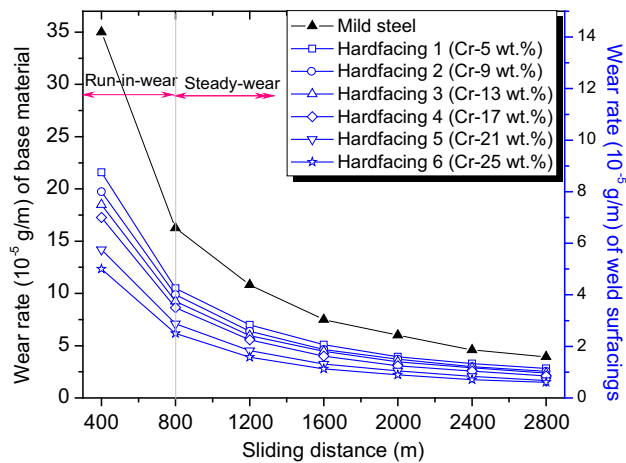


Fig. 4 Typical wear rate characteristics of substrates and weld surfacing w.r.t. sliding distance

mechanical and the interfacial bonding of the carbides with the matrix. The good interfacial bonding is attributed to the addition of manganese, whose effect is to make the matrix tough enough to prevent fragmentation of carbides during sliding. The results of decreased wear rate with the increase in the number of carbides are consistent with the earlier work reported by various authors for different materials [4, 5, 32, 37]. When compared to 25 wt% chromium addition, rest of the hardfacings exhibit lesser area fraction of carbide particles, therefore the wear of matrix regions exposed to the counter surface will be excessive. In view of this, Chatterjee and Pal [50] reported that if the preferential wear of matrix region is more, the carbides become unsupported and susceptible to spalling and fracture. From the present investigation, each element has been found to play a key role in enhancing the material's properties. Crespo et al. [51] also stated that no compound alone can improve the performance of the weld surfacings and a correct composition of elements must be there to balance the operational characteristics of the process.

4 Conclusions

In this research, six different chromium additive hardfacings were developed by using SMAW process. The increase in chromium content was found to be beneficial in increasing the area fraction of carbides which in turn increased the hardness of hardfacings and suggested that hardness was dependent on the area fraction of carbides. Hardfacing containing 17 wt% chromium exhibited the appearance of long spine-like and hollow hexagons, which got refined with the increase of chromium from 17 to 25 wt%. The refined microstructure with the increase of chromium content played an important role in enhancing the wear resistance of hardfacings, hence, high chromium content offered better wear resistance in comparison to substrate and other chromium additive hardfacings. The correlation between hardness and wear resistance exhibited that the bulk hardness was a true index of the wear resistance and proved to be a key factor to be evaluated while comparing wear resistance of iron-based hardfacings.

Acknowledgments The authors are thankful to Mr. Shiv Kumar for his assistance during SEM.

References

- Berns H, and Fischer A, *Metallography* **20** (1987) 401.
- Henderson J L, and Bulloch J H, *Int J Press Vessel Pip* **57** (1994) 253.
- Crespo A C, Scotti A, and Perez M R, *J Mater Process Technol* **199** (2008) 265.
- Chang C M, Chen Y C, and Wu W, *Tribol Int* **43** (2010) 929.
- Fan C, Chen M C, Chang C M, and Wu W, *Surf Coat Technol* **201** (2006) 908.
- Chang C M, Lin C M, Hsieh C C, Chen J H, and Wu W, *J Alloys Compd* **487** (2009) 83.
- Azimi G, and Shamanian M, *J Alloys Compd* **505** (2010) 598.
- Azimi G, and Shamanian M, *J Mater Sci* **45** (2010) 842.
- Sabet H, Khierandish S, Mirdamadi S, and Goodarzi M, *Tribol Lett* **44** (2011) 237.
- Coronado J J, Caicedo H F, and Gomez A L, *Tribol Int* **42** (2009) 745.
- Singla Y K, Dwivedi D K, and Arora N, in *23rd International Conference on Processing and Fabrication of Advanced Materials (PFAM 2014)*, IIT Roorkee (2014), p 674.
- Correa E O, Alcantara N G, Valeriano L C, Barbedo N D, and Chaves R R, *Surf Coat Technol* **276** (2015) 479.
- Correa E O, Alcantara N G, Tecco D G, and Kumar R V, *Metall Mater Trans A* **38** (2007) 1671.
- Correa E O, Alcantara N G, Tecco D G, and Kumar R V, *Metall Mater Trans A* **38** (2007) 937.
- Dogan H, Findik F, and Oztarhan A, *Ind Lubr Tribol* **55** (2003) 76.
- Dogan H, Findik F, and Oztarhan A, *Ind Lubr Tribol* **56** (2004) 341.
- Kiratli N, and Findik F, *Ind Lubr Tribol* **63** (2011) 127.
- Lin Y C, and Wang S W, *Tribol Int* **36** (2003) 1.
- Svensson L E, Gretoft B, Ulander B, and Bhadeshia H K D H, *J Mater Sci* **21** (1986) 1015.
- Berns H, and Fischer A, *Mater Charact* **39** (1997) 499.
- Zhang A F, Xing J D, Fang L, and Su J Y, *Wear* **257** (2004) 198.
- Zumgahr K H, *Microstructure and Wear of Materials*, Elsevier, Amsterdam (1987).
- Turenne S, Lavallee F, and Masounave J, *Mater Sci* **24** (1989) 3021.
- Noble D N, *Mater Constr* **17** (1985) 605.
- Fiore N, Antony K C, and Kosel T H, in *Proceedings of international conference on Corrosion–Erosion Wear of Materials in Emerging Fossil, Energy Systems NACE, USA, Houston, TX (1982)*, p 266.
- Atamert S, and Stekly J, *Surf Eng* **9** (1993) 231.
- Berns H, and Fischer A, *Wear* **112** (1986) 163.
- Badisch E, Kirchgäßner M, Polak R, and Franek F, *Triobotest* **14** (2008) 225.
- Kirchgäßner M, Badisch E, and Franek F, *Wear* **265** (2008) 772.
- Dasgupta R, Thakur R, Yadav M S, and Jha A K, *Wear* **236** (1999) 368.
- ASTM G99–05 Standard, *Standard Test Method for Wear Testing with a Pin-on-Disk Apparatus*, (2010).
- Kazempour M, Shokrollahi H, and Sharafi S, *Tribol Lett* **39** (2010) 181.
- Powell G L F, Carlson R A, and Randle V, *J Mater Sci* **29** (1994) 4889.
- Buchanan V E, Shipway P H, and McCartney D G, *Wear* **263** (2007) 99.
- Buchanan V E, McCartney D G, and Shipway P H, *Wear* **264** (2008) 542.
- Buchanan V E, *Surf Coat Technol* **203** (2009) 3638.
- Chang C M, Chen L H, Lin C M, Chen J H, Fan C M, and Weite W, *Surf Coat Technol* **205** (2010) 245.
- Ohide T, and Ohira G, *Foundry* **76** (1983) 7.
- Buchely M F, Gutierrez J C, Leon L M, and Toro A, *Wear* **259** (2005) 52.
- Winkelmann H, Badisch E, Kirchgäßner M, and Danninger H, *Tribol Lett* **34** (2009) 155.
- Badisch E, Katsich C, Winkelmann H, Franek F, and Roy M, *Tribol Int* **43** (2010) 1234.

42. Sapate S G, and Rao A V R, *Wear* **256** (2004) 774.
43. Katsich C, Badisch E, Roy M, Heath G R, and Franek F, *Wear* **267** (2009) 1856.
44. Li D, Liu L, Zhang Y, Ye C, Ren X, Yang Y, and Yang Q, *Mater Des* **30** (2009) 340.
45. Atamert S, and Bhadeshia H K D H, *Mater Sci Eng A* **130** (1990) 101.
46. Sapate S G, and Rao A V R, *Tribol Int* **39** (2006) 206.
47. Junfeng G, Lu P, You W, Saiyue L, and Zhiwei Z, *Appl Surf Sci* **360** (2016) 849.
48. Sharma V, Kumar S, Panwar R S, and Pandey O P, *J Mater Sci* **47** (2012) 6633.
49. Viafara C C, and Sinatora A, *Wear* **271** (2011) 1689.
50. Chatterjee S, and Pal T K, *Wear* **255** (2003) 417.
51. Crespo A C, Fuentes R F, and Scotti A, *J Mater Eng Perform* **19** (2010) 685.